9th AUSTRALASIAN
FLUID MECHANICS CONFERENCE,
AUCKLAND, 8-12 DECEMBER 1986

Further Investigations of the Aerodynamics of Floatation Ovens

M. J. DAVIES[1] and D. H. WOOD[2]

[1]Research & Technology Centre, BHP Steel Coated Products Division.
[2]Department of Mechanical Engineering, University of Newcastle, Australia.

ABSTRACT

This paper presents an extension of the study of the aerodynamics of floatation ovens. These ovens contain nozzles that are the two-dimensional analogue of hovercraft. The floatation nozzles support and heat continuous metal strip that has been painted on both surfaces. Results show that initial jet velocity profiles are non-uniform because of curvature effects. Measurements of the wall shear stress on a flat plate, representing the strip, show that the theory developed by Davies & Wood (1983a) is justified in neglecting its contribution. The quasi-steady assumption, that the lift from a floatation nozzle is nearly proportional to the inverse of the distance from the nozzle to the strip, is used to develop a model to predict the location of the strip in the oven.

INTRODUCTION

Floatation ovens are used by modern continuous strip paint lines to dry and cure thin metal strip that has been simultaneously coated on both surfaces. The floatation oven supports or floats the strip to prevent damage to the coated surfaces and heats the strip to a temperature required to cure the paint film.

The basic component of the floatation oven is a nozzle shown schematically in Figure 1. Floatation nozzles are located above and below the strip along part of the oven length. Only one half of the upper nozzle is shown in Figure 1 because the upper and lower nozzles are similar and each nozzle is symmetric about the centre line. A floatation nozzle is the two-dimensional analogue of hovercraft.

Simple hovercraft theory assumes that the inviscid jet exits from the nozzle with constant velocity and then deflects with a constant radius of curvature, r_o. From the geometry of Figure 1

$$r_o = h/(1+\cos\theta). \qquad (1)$$

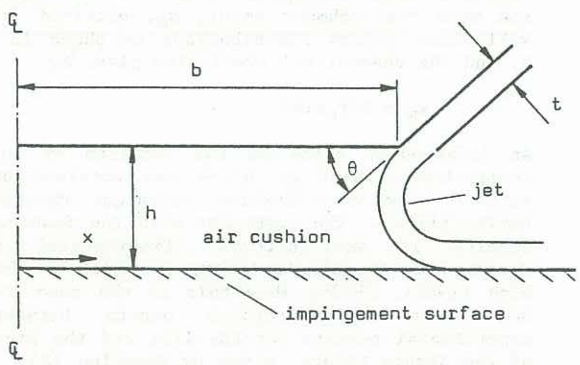

Figure 1 Half-sectional view of upper floatation nozzle

The theory shows that the lift varies with the inverse of the distance between the strip and the floatation nozzle. The lift per unit length of jet, L, is given by

$$L/2 = P_c b + J\sin\theta \qquad (2)$$

where P_c is the gauge cushion pressure given by

$$P_c = J/r_o \qquad (3)$$

and J is the jet momentum flux per unit length of jet. Davies & Wood (1983a) showed that the simple theory produced remarkably accurate estimates of the lift when compared to experimental results. The good agreement was explained by showing that the simple theory is an approximate solution to the Navier-Stokes equations. The most significant restriction of both the simple theory and the analysis of Davies & Wood (1983a) is that the radius of curvature of the jet path must remain nearly constant.

Davies & Wood (1983b) investigated aspect ratio effects in floatation nozzles and found that, at sufficiently low aspect ratios, there was a range of floatation heights, h, over which the lift on the strip increased with the distance from the nozzle to the strip. It was argued by Davies & Wood (1983b) that the main effect of a low aspect ratio is to allow a form of 'communication' between the two jets over their entire length. If this communication is weakened by installing vortex generators at the exit of each jet (strings placed over the slots at regular intervals across the nozzle span) to destroy any spanwise coherence of the jets, the resulting lift becomes qualitatively similar to that of a nozzle with an 'infinite' aspect ratio.

The purpose of this paper is to extend the experimental knowledge of floatation nozzles and to use the results to develop a mathematical model of steady state strip behaviour in a floatation oven.

EXPERIMENTAL RESULTS

Experiments were performed on a scale model fitted to a wind tunnel. The two jets that emerged from the floatation nozzle impinged onto a flat plate. The fan speed was fixed while the plate was moved through a range of h, so that J varied with h.

Jet mean velocity profiles were measured to calculate J and to check the uniformity of flow at the nozzle exit. Measurements were made with a 5 μm single hot wire probe and a home made constant temperature anemometer, similar to that described by Perry (1982). Full details of the experimental techniques are given in Davies (1986).

Typical jet velocity profiles, measured at the centre line of the nozzle span, are shown in Figure 2; x' is parallel to x and about 0.5 mm downstream of the nozzle exit, but with an arbitrary origin that was constant for all h/t. As shown by the magnitude of the velocities at either side of the nozzle outlet there is negligible entrainment into

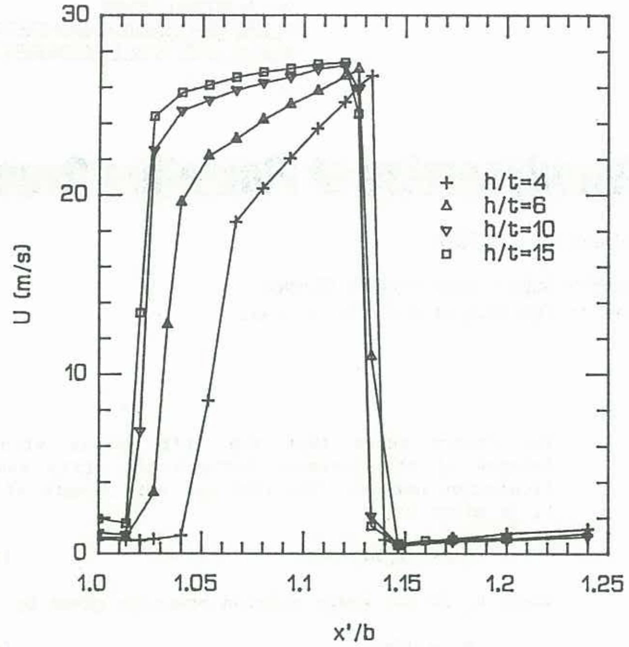

Figure 2 Typical jet velocity profiles

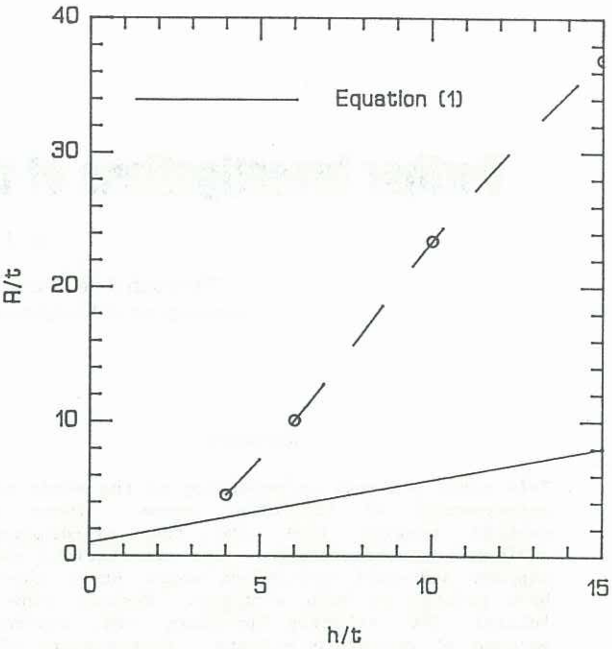

Figure 3 Comparison of the initial radius of curvature with the radius of curvature predicted by the simple theory.

the jets. The profiles become more uniform and 'fill out' as h/t increases.

The non-uniformity of the initial jet velocity profiles can be attributed to the effect of curvature of the jet. Consider a two-dimensional inviscid flow field consisting of an initial straight section followed by a curved section of inner radius R. The straight section of the flow has a constant velocity distribution so all the streamlines have the same Bernoulli constant. The bend in the curved section of the flow will induce a radial pressure gradient given by

$$(1/\rho)\ \partial P/\partial r = U^2/r. \tag{4}$$

where ρ is the density, P is the pressure, r is the radius and U is the velocity.

Differentiating Bernoulli's equation with respect to r and using Equation (4) gives

$$\partial U/\partial r = -U/r \tag{5}$$

so that U will decrease as r increases by an amount that depends on r. The solution to Equation (5) is

$$U = C/(R+y) \tag{6}$$

where C is a constant and y is in the direction of R and is measured from the inner streamline. This direction was assumed to lie in the direction of t in Figure 1. The values of y were obtained as the distance from the inner streamline in the direction of x' divided by $\sin\theta$.

Figure 3 shows the value of R inferred from the velocity profiles of Figure 2 using Equation (6). Comparison of the initial radius of curvature, R, with the theoretical prediction of the radius of curvature, given by Equation (1), is shown. It is to be expected that $r_o < R$ because the radius of curvature is infinite upstream of the nozzle outlet and presumably reduces to r_o at some point downstream. Results show that, at least for small values of h/t, U cannot be uniform at the nozzle exit, even for inviscid flow, because of curvature effects. Thus the simple theory is internally inconsistent, but the more general analysis of Davies & Wood (1983a) is not restricted to uniform exit velocity profiles.

The wall shear stress, τ_w, was measured because both the simple theory and the analysis of Davies & Wood (1983a) ignored its effect. Measurements were made using a Stanton probe in the form of a razor blade segment, of thickness 0.2 mm, positioned over a static pressure hole. The main reasons for choosing the Stanton probe were (i) minimization of the gauge height, (ii) standard calibrations are readily available and easily handled, and (iii) ease of construction over other devices such as a surface fence. Full experimental techniques are given in Davies (1986).

A typical distribution of the wall shear stress, for h/t=4, measured at the centre line of the nozzle span, is shown in Figure 4. It should be noted that (i) the magnitude of $-\tau_w$ will not necessarily be correct, since the Stanton probe was not calibrated for $\tau_w < 0$ and (ii) τ_w is close to zero at the centre line (x=0). Results prove (not shown) that the contribution of the wall shear stress to an x-direction momentum balance is small as assumed by Davies & Wood (1983a).

The distribution of τ_w in the region $x/b < 1$ suggests a double mean vortex pattern in the cushion region, rather than a single vortex that was expected. Results at other values of h/t (not shown) suggest a similar behaviour.

Figure 5 shows a comparison between the location of the mean reattachment point, x_m, obtained from the wall shear stress distributions as shown in Figure 4, and the theoretical prediction given by

$$x_m = b + r_o \sin\theta. \tag{7}$$

An independent check on the location of the mean reattachment point at h/t=4 was obtained using a surface flow visualization technique described by Davies (1986). The agreement with the Stanton probe results is satisfactory. Experimental results depart from the simple theory for h/t> 4. Davies & Wood (1983a, 1983b) show this is the same range of h/t where a discrepancy occurs between the experimental results for the lift and the prediction of the simple theory, given by Equation (2). Davies & Wood (1983a) attributed this discrepancy to a rapid change in the radius of curvature as the jet approached the plate. This suggestion is consistent with the results in Figure 5.

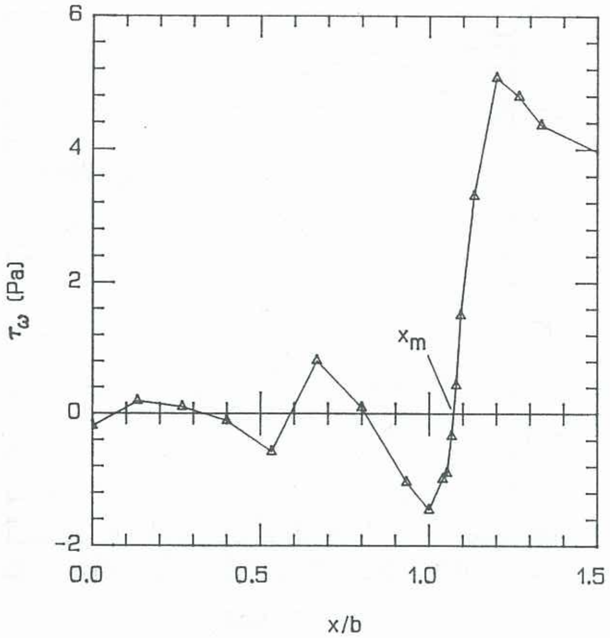

Figure 4 Distribution of wall shear stress for h/t=4.

A result (not shown) is that, although L is approximately proportional to 1/h, the interaction with the fan characteristic gives L as proportional to $h^{-0.6}$.

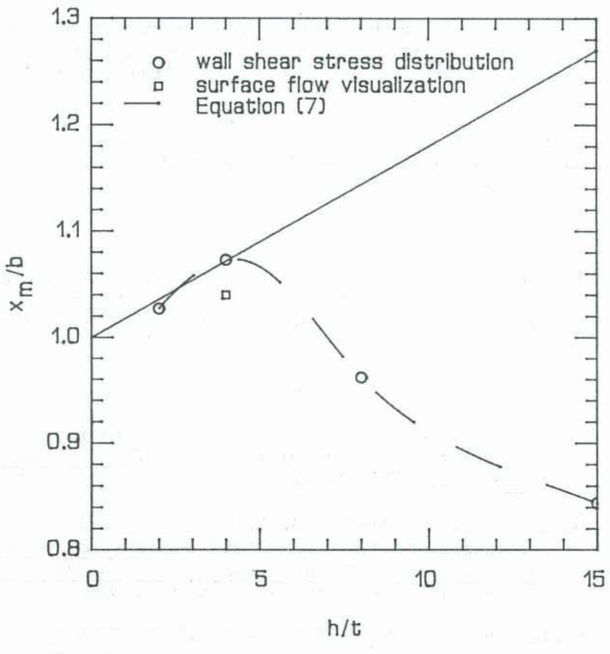

Figure 5 Location of the mean reattachment point.

MATHEMATICAL MODELLING OF THE STRIP AERODYNAMICS

An important consideration in the design or optimization of a floatation oven is the ability of the strip to be located in the oven so that the painted surfaces do not contact the nozzles and damage the product. Typical floatation ovens consist of a catenary section (comprising an initial flow-out period after coating and an oven region in which most of the solvents are evaporated from the paint film) where the strip is suspended under its own weight and a floatation section where the strip is supported, horizontally, between the upper and lower arrays of floatation nozzles. Therefore, it is desirable to predict the location of the strip, relative to the nozzles, for a given set of line conditions, such as strip tension and strip thickness, to ensure that the transition of the strip through the catenary section and into the floatation section will not result in damage to the painted surfaces.

For a preliminary analysis, the following assumptions are made.

(i) Bending stresses are neglected because the strip thickness is small compared to the strip length.

(ii) The jet velocity for all lower floatation nozzles is a constant value and the same is true for the upper floatation nozzles.

(iii) The gap between the lower and upper arrays of floatation nozzles is constant along the oven length.

(iv) The lift of a floatation nozzle is of the form of Equation (2).

(v) The lift is localized at the centre of the nozzle and is constant across the span.

(vi) Steady state behaviour is considered.

Considering a free body diagram of the strip it is easy to show (for small dy/dx)

$$T\, d^2y/dx^2 + F = 0 \qquad (8)$$

where T is a constant strip tension, y is the vertical location of the strip with respect to an arbitrary datum, x is the distance measured along the oven length and F is the net vertical force on the strip per unit length. In the catenary section of the oven F is only a function of the strip weight, however, in the floatation section of the oven F is a function of the strip weight and the lifts generated by the floatation nozzles above and below the strip.

Because of assumption (iv), Equation (8) leads to a second order, non-linear, differential equation for the floatation section of the oven. Equation (2) shows that the lift on the strip from a floatation nozzle is of the form

$$L = A/y + B \qquad (9)$$

where A and B are constants and y is the distance measured from the nozzle to the strip. The term A/y represents the contribution from the gauge cushion pressure acting over the area between the jets and B represents the contribution from the vertical component of jet momentum flux, and usually A/y>> B. Values of A and B were obtained using Equation (2) and estimates of the air flow rates into the oven. Assuming the x-axis is at the level of the upper array of floatation nozzles (that is, y is negative), the net vertical force per unit length of strip, F, is given by

$$F(y) = A_l/(D+y) + B_l + A_u/y - B_u - W \qquad (10)$$

where A_l and B_l are constants related to the lower array of floatation nozzles, A_u and B_u are constants related to the upper array of floatation nozzles, D is the gap between the upper and lower arrays of floatation nozzles and W is the strip weight per unit length.

Equation (8) is subject to boundary conditions on the strip location, y, at each end of the floatation oven. A numerical scheme is used to solve Equation (8), in conjunction with Equation (10) and the boundary conditions, at discrete points (each nozzle pair) along the oven length. The scheme involves representing the second derivative, in Equation (8), by the finite difference approximation and using the simple Newton iteration to solve, numerically, the resulting tridiagonal matrix system of algebraic equations for the strip location. The numerical scheme requires an initial estimate of the strip location.

Figure 6 shows typical theoretical predictions of the strip location in a floatation oven for a constant strip tension of T=25 kN and strip thickness, H, of 0.6, 1 and 1.4 mm. Both the distance of the strip below the first upper floatation nozzle and the distance of the strip below the last upper floatation nozzle increase as the strip thickness is increased.

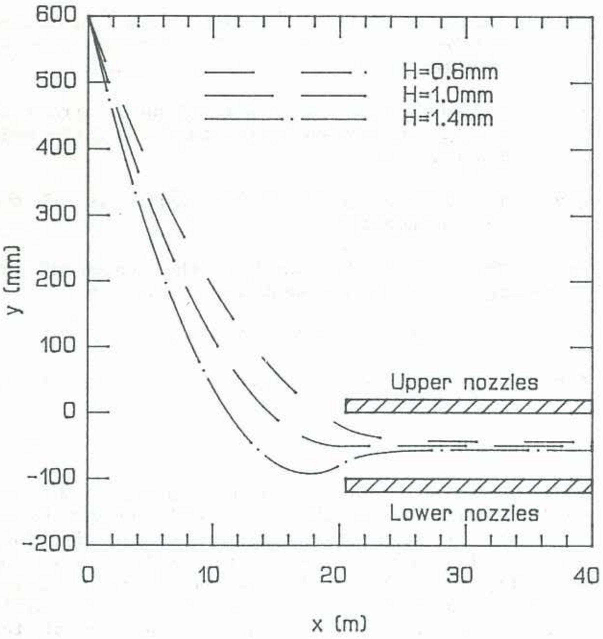

Figure 6 Prediction of the strip location for various strip thicknesses and a constant strip tension (T=25 kN).

Figure 7 shows the distance of the strip below the first upper floatation nozzle, y_t, as a function of strip thickness, H, for various values of the strip tension, T. For T=5 kN and H >0.63 mm the model predicts that the strip will make contact with the lower catenary nozzles. Figure 7 indicates the range of strip thickness, H, for a given strip tension, T, if limits were set on y_t. For example, if $-70 \leq y_t \leq -30$ mm and T=25 kN then $0.7 \leq H \leq 1.3$ mm.

CONCLUSIONS

Results show that the simple 'hovercraft' theory of floatation nozzles is reasonably accurate for $h/t < 4$, but that the velocity profile is not constant at the nozzle exit, due to curvature effects, particularly at small values of h/t. Measurements of the wall shear stress show that the simple theory and the analysis of Davies & Wood (1983a) are justified in ignoring its effect. The mean reattachment point obtained from the wall shear stress distributions agreed well with that from an

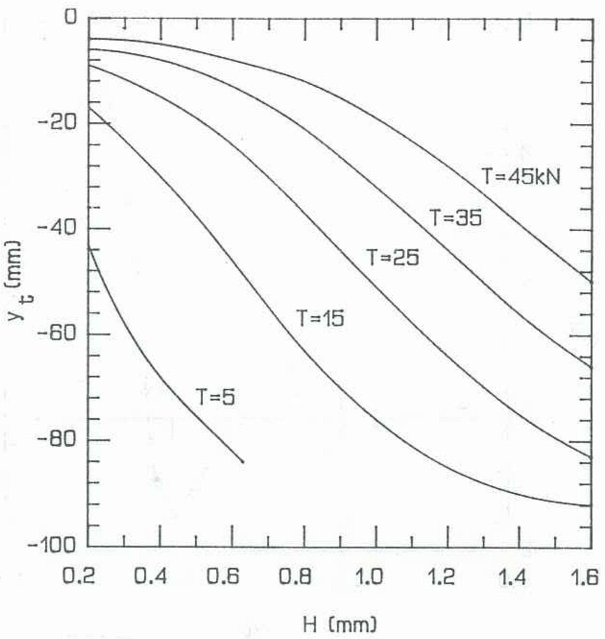

Figure 7 Prediction of the strip location below the first upper floatation nozzle as a function of strip thickness and strip tension.

independent flow visualization technique at one value of h/t. As h/t increases the mean reattachment point deviates significantly from that given by the simple theory.

A mathematical model has been developed to predict the steady state location of continuous strip between floatation nozzles in an actual floatation oven.

Further work will involve extending the steady state analysis to a time dependent analysis of the strip behaviour.

ACKNOWLEDGEMENT

The authors wish to thank the management of BHP Steel International Group, Coated Products Division, for permission to publish the information contained in this paper.

REFERENCES

Davies, M.J. and Wood, D.H. (1983a): The basic aerodynamics of floatation. ASME J. Fluids Eng., Vol. 105, 323-328.

Davies, M.J. and Wood, D.H. (1983b): Aspect ratio effects of floatation systems. Proc. of the 8th Australasian Fluid Mechanics Conference, 3C.9-3C.12, University of Newcastle, NSW.

Davies, M.J. (1986): Aerodynamics of continuous strip paint line floatation ovens. ME Thesis. University of Newcastle, NSW.

Perry, A.E. (1982): Hot Wire Anemometry. Clarendon Press, Oxford.